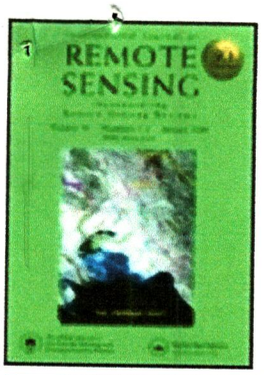

(4)

International Journal of Remote Sensing

ISSN: 0143-1161 (Print) 1366-5901 (Online) Journal homepage: http://www.tandfonline.com/loi/tres20

Interannual variation of bigeye tuna (Thunnus obesus) hotspots in the eastern Indian Ocean off Java

Mega Syamsuddin, Sei-Ichi Saitoh, Toru Hirawake, Fadli Syamsudin & Mukti Zainuddin

To cite this article: Mega Syamsuddin, Sei-Ichi Saitoh, Toru Hirawake, Fadli Syamsudin & Mukti Zainuddin (2016): Interannual variation of bigeye tuna (Thunnus obesus) hotspots in the eastern Indian Ocean off Java, International Journal of Remote Sensing, DOI: 10.1080/01431161.2015.1136451

To link to this article: http://dx.doi.org/10.1080/01431161.2015.1136451

Published online: 19 Jan 2016.

Interannual variation of bigeye tuna (Thunnus obesus) hotspots in the eastern Indian Ocean off Java

Article *in* International Journal of Remote Sensing · January 2016

DOI: 10.1080/01431161.2015.1136451

CITATIONS
32

READS
581

5 authors, including:

Mega Syamsuddin
Universitas Padjadjaran
40 PUBLICATIONS **265** CITATIONS
SEE PROFILE

Sei-Ichi Saitoh
Hokkaido University
225 PUBLICATIONS **4,862** CITATIONS
SEE PROFILE

Toru Hirawake
National Institute of Polar Research
144 PUBLICATIONS **1,929** CITATIONS
SEE PROFILE

Fadli Syamsudin
Badan Pengkajian dan Penerapan Teknologi
80 PUBLICATIONS **1,740** CITATIONS
SEE PROFILE

International Journal of Remote Sensing, 2016
http://dx.doi.org/10.1080/01431161.2015.1136451

Taylor & Francis
Taylor & Francis Group

Interannual variation of bigeye tuna (*Thunnus obesus*) hotspots in the eastern Indian Ocean off Java

Mega Syamsuddin[a]*, Sei-Ichi Saitoh[b], Toru Hirawake[b], Fadli Syamsudin[c], and Mukti Zainuddin[d]

[a]*Faculty of Fisheries and Marine Science, Padjadjaran University, Bandung, Indonesia;* [b]*Faculty of Fisheries Sciences, Hokkaido University, Hakodate, Japan;* [c]*The Agency for the Assessment and Application of Technology (BPPT), Jakarta, Indonesia;* [d]*Faculty of Marine Science and Fisheries, Hasanuddin University, Makassar, Indonesia*

(*Received 31 December 2014; accepted 20 December 2015*)

Remotely derived environmental variables, including sea surface height anomaly (SSHA), sea surface temperature (SST), chlorophyll-*a* (chl-*a*), eddy kinetic energy (EKE), mixed layer data set of argo float (MLD), Niño 3.4 index, and bigeye tuna catch data for the period 1997–2008, were used to analyse ocean climate variability and how they relate to the hotspots of bigeye tuna catch in the eastern Indian Ocean off Java. The empirical orthogonal function (EOF) was performed to obtain a more detailed structure of the spatio-temporal ocean variability in the region. The results showed that the first EOF modes of chl-*a*, SSHA, and SST accounted for 42.8%, 36.5%, and 27.4% of total variance, respectively, and these corresponded to the interannual signal. The maps of spatial patterns of the first EOF modes of SSHA, SST, and chl-*a* gave very typical values for cold-water SSHA, low SST, and high chl-*a* concentration along the southern coast of the Indonesian archipelago; and warm-water SSHA, high SST, and low chl-*a* concentration in the offshore region to make frontal areas along the latitudinal line around 10–12° S. The EOF analysis further revealed a strong relationship between the El Niño event and favourable oceanographic conditions, resulting in a significant increase in bigeye tuna catch. The average hook rate of 0.71 (0.43) was recorded during El Niño (La Niña). Major hotspots were located away from the confluence region and frontal areas around 11–16° S and 110–118° E and were thus demonstrated as the most favourable oceanographic conditions for bigeye tuna fishing in the eastern Indian Ocean off Java.

1. Introduction

The Indian Ocean supports the second largest tuna fishery in the world after the Pacific Ocean, contributing 24% of the global total (Miyake et al. 2010). Bigeye tuna (*Thunnus obesus*) is a commercially targeted species and represents one of the most valuable components of longline fisheries in the eastern Indian Ocean (EIO; ISSF 2012). Bigeye tuna is a productive tropical species that accounts for more than 10% of the total catch of market tuna species worldwide (Miyake et al. 2010). Bigeye tuna generally prefer water temperatures between 17 and 22°C. They prefer to stay near, and usually below, the thermocline and come to the surface periodically (Pepperell 2010). In the upper water

* Corresponding author. Email: vegha16@yahoo.com Faculty of Fisheries and Marine Science, Padjadjaran University, Jalan Raya Bandung-Sumedang KM 21, Jatinangor, Bandung 40600, Indonesia

column at night, bigeye tuna prefer a thermal range of 22–26°C (Bigelow, Hampton, and Miyabe 2002). The main depth range of fishing for bigeye tuna in the Indian Ocean is 161–280 m (Mohri and Nishida 1999), although they can inhabit the depth range 0–100 m at night (Howell, Hawn, and Polovina 2010).

The EIO off Java is a region where currents and wave systems make conditions ideal for good fishing zones or hotspots. The Indonesian Throughflow (ITF), which is the outflow from the Pacific to the Indian Ocean through the Lombok and Ombai Straits; the Timor Passage (Gordon 2005); and the seasonally reversing South Java Current (SJC) along the southern coast of the Indonesian seas (Sprintall et al. 2010) all meet the Indian Ocean Kelvin Waves (IOKWs), which are also propagated along this area on the southern coast of Indonesian seas (Syamsudin, Kaneko, and Haidgovel 2004). Offshore, the Indian Ocean South Equatorial Current (SEC) enters the region from the southern Indian Ocean off southern Java (Zhou, Murtugudde, and Jochum 2008) and the westerly Rossby Waves (RWs) propagate along the latitudes 12–15° S, as shown in Figure 1(*b*) (Gordon 2005; Sprintall et al. 2009). The ITF and IOKWs have strong interannual signals related to the El Niño–Southern Oscillation (ENSO) (Ffield et al. 2000), and the SJC also influences the surrounding areas on seasonal time scales (Sprintall et al. 1999).

The Indonesian seas are the only major low-latitude connection in the global oceans (Sprintall et al. 2009). This connection permits the transfer of Pacific waters to the Indian Ocean by the ITF. As a result, the ITF plays an important role in the climatic system (Gordon 2005). Interannual signals in the ITF are therefore formed by interannual variability associated with ENSO (Potemra and Schneider 2007). ENSO exerts an adverse effect on *T. obesus* catch globally (Lehodey 2001; Howell and Kobayashi 2006), and therefore understanding the effects of ocean climate variability on bigeye tuna distribution is an essential step towards sustainable management of tuna resources in the EIO off Java.

The effects of ENSO climate variability on oceanographic conditions and tuna catch in the Pacific have been reported widely (Lehodey et al. 1997; Howell and Kobayashi 2006; Torres-Orozco et al. 2006; Briand, Brett, and Patrick 2011), but are less studied in the Indian Ocean. Most Indian Ocean studies have focused on the oceanographic variability in the interior Indonesian seas (Zhou, Murtugudde, and Jochum 2008; Sprintall et al. 2009), the correlation of individual oceanographic factors with ENSO (Yoder and Kennely 2003), and ocean colour variability in the Indonesian seas (Susanto, Moore, and Marra 2006; Iskandar, Rao, and Tozuka 2008). In this study we analysed oceanographic parameters, including sea surface height anomaly (SSHA), sea surface temperature (SST), chlorophyll-*a* (chl-*a*), and eddy kinetic energy (EKE) in order to examine ocean climate variability and how they relate to the hotspots of bigeye tuna fishing in the EIO off Java. This research is not only important for scientific development, but also for sustainable fisheries management in the EIO.

2. Materials and methods

A time series of bigeye tuna catch data was collected from longline fishing logbooks provided by the Indonesian Government Incorporated Company of Perikanan Nusantara at Benoa, Bali, Indonesia. From this data set, the catch rate of bigeye tuna was expressed as a percentage of hook rate (HR), which was calculated as the number of fish caught per 100 hooks and integrated into weekly and monthly fishing activity. HR, therefore, shows how many tuna were hooked per unit of 100 longline hooks and denotes catch per unit effort.

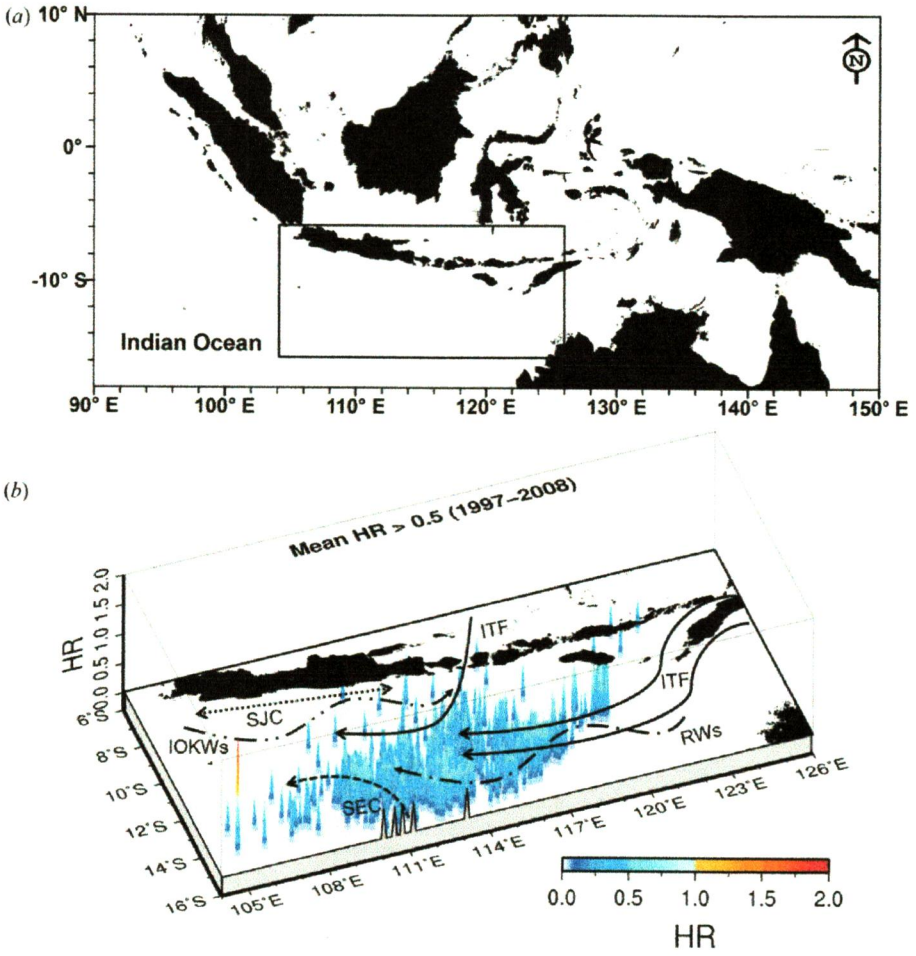

Figure 1. (*a*) Map of the Indonesian seas, with the inset box representing the study area in the eastern Indian Ocean (EIO) off Java. (*b*) Bigeye tuna hotspots (HR > 0.5) during the period 1997–2008 (blue bars) overlaid with the wave and current systems in the EIO off Java, indicated by the dotted line for the South Java Current (SJC) and solid lines for the Indonesian Throughflow (ITF); the line with dashes and two dots denotes the Indian Ocean Kelvin Waves (IOKW), the line with dashes and one dot denotes the Rossby Waves (RW), and the dashed line denotes the Indian Ocean South Equatorial Current (SEC). The colour bar denotes HR values.

In situ data of conductivity, temperature, and depth (CTD) were obtained from the Indonesian RV 'Baruna Jaya' of the Agency for the Assessment and Application of Technology (BPPT), Indonesia. Measurements were taken in February 2000 (La Niña). Additional CTD data were used for comparison to the El Niño events during the period June 2002–June 2006. The data were obtained from a mixed-layer data set (MLD) of the Argo float programme from the Japan Agency for Marine-Earth Science and Technology (JAMSTEC).

Remotely derived oceanographic variables included SSHA, SST, chl-*a*, and EKE. SSHA data had spatial and temporal resolution of 1/3° and 7 days, respectively, and were taken for the period January 1997–December 2008 from TOPEX and Poseidon ERS-1/2

altimeters (http://www.aviso.oceanobs.com). The SSHA data are produced and distributed by Archiving, Validation and Interpretation of Satellite Oceanographic Data (AVISO).

The SST data had spatial and temporal resolution of 4 km and 7 days, respectively, and were derived for the period January 1997–December 2008 from the Advanced Very High Resolution Radiometer (AVHRR) sensor on board the National Oceanic and Atmospheric Administration (NOAA) satellite, as a product of the Physical Oceanography Distributed Active Archive Center (PODAAC; http://podaac.jpl.nasa.gov) of the Jet Propulsion Laboratory (JPL)/National Aeronautics and Space Administration (NASA).

We obtained daily composite cycles of chl-*a* data to calculate weekly mean (7 days) chl-*a*. Chl-*a* data from the Moderate Resolution Imaging Spectroradiometer (MODIS) and SeaWiFS with spatial resolution of 9 km were downloaded from OceanColor (http://oceancolor.gsfc.nasa.gov) for the period September 1997–December 2008.

In regard to EKE, the weekly global geostrophic current velocity images from AVISO were averaged to monthly data for the *u* and *v* components with a spatial resolution of 1/3°. The *u* and *v* components are, respectively, zonal and meridian geostrophic components related to SSHA. The *u* and *v* rasters were used to calculate EKE using the equation introduced by Robinson (2004):

$$\mathrm{EKE} = 1/2\left(u^2 + v^2\right). \tag{1}$$

For data analysis, all weekly images of SSHA, SST, chl-*a*, and EKE were averaged to monthly data using SeaDAS VA 6.1 and resampled to match with the chl-*a* spatial resolution (9 km) using ArcGIS 9.3 software.

The Niño 3.4 index was used as a proxy to the climatic conditions of ENSO. The Niño 3.4 index is the averaged sea surface temperature anomaly in the region bounded by 5° N–5° S, from 120°–170° W. The index is available from the NOAA Climate Prediction Center (http://www.cpc.ncep.noaa.gov). El Niño and La Niña events are identified when the five-month running average of the Niño 3.4 index exceeds +0.5°C for El Niño and −0.5°C for La Niña for at least five consecutive months.

In this research, the bigeye tuna catch and satellite remotely sensed data were analysed for the 12 years of data sets for January 1997–December 2008 to determine the differences in regional climatic conditions during strong (1997), moderate (2002), and weak (2006) El Niño events, strong (1999) La Niña events, and normal year (2005) events. In the analysis, the fishing locations were overlaid with the oceanographic variables within 9 km spatial resolution in order to give a better representation of oceanographic parameter changes on the coarse grid of bigeye tuna catch rates.

The empirical orthogonal function (EOF) was performed to obtain a more detailed structure of spatio-temporal ocean variability. EOF analysis is a useful technique for decomposing a time series of geophysical data into temporal and spatial variability in terms of orthogonal functions, or statistical modes. EOF analysis has been commonly used to describe spatio-temporal ocean variability (Polovina and Howell 2005; Iida and Saitoh 2007). EOF analysis was applied to the raw weekly data set of SSHA and SST and monthly data of chl-*a* (because of a lack of data in many of the weekly images) over the whole study area in order to decompose total variability into major modes associated with interannual and seasonal variability. Here, we examined only the first and second dominant modes with higher variance that may have significant physical meaning and statistical independence according to the criteria given by Kelly (1988). Eigenvalues with

contribution rates over 5% are considered significant for the 95% confidence limit. A more comprehensive explanation of the concept of EOF analysis has been provided by Bjornsson and Venegas (1997). On the basis of the results for EOF, the maps of spatial and temporal patterns of ocean variability in the EIO off Java were particularly useful to distinguish ENSO events.

3. Results

3.1 *Temporal variability of bigeye tuna catches*

Figure 2 shows significant variations in HR during the study period. The peak season of bigeye tuna catch rates was found to be May–July 1997 (HR: 0.87–0.94), May–August 2001 (HR: 1.32–1.9), June–August 2002 (HR: 1.06–1.66), and May–July 2003 (HR: 0.64–0.86). The maximum bigeye tuna catches occurred in June 1997 (HR: 0.92), August 2001 (HR: 1.9), and June 2002 (HR: 1.66). Notably, HR seemed to increase during positive Niño 3.4 indices as shown by these values above, where higher values were observed during strong (1997) and moderate (2002) El Niño events. However, higher HR in May–August 2001 and May–July 2003 was noted in the absence of any El Niño event. To investigate these periods of higher HR, we considered that besides ENSO, the EIO off Java is also influenced by the climatic event of the Indian Ocean dipole (IOD), an internal air–sea coupling in the tropical Indian Ocean. Extreme IOD events are characterized by strong cooling in the EIO (Saji et al. 1999). Intensity of the IOD is represented by the dipole mode index (DMI), which is an anomalous SST gradient between the western equatorial Indian Ocean (50–70° E and 10°S–10° N) and the southeastern equatorial Indian Ocean (90–110° E and 10°S–0° N). This index is available from JAMSTEC (www.jamstec.go.jp). Positive DMI indicates cooling SST in the southeastern Indian Ocean that can cause drying impacts similar to El Niño in the Pacific Ocean. The year 2003 is categorized as a positive IOD phase, with DMI values ranging from 0.6–0.9°C (Rao et al. 2009). The year 2001 is not categorized as a positive IOD phase because the SST anomaly (DMI) did not reach or approach 0.5°C during three consecutive months, but DMI values were in a positive range 0.26–0.55°C during May–August 2001. This could explain why SST was cooler during those periods and there were oceanographic conditions conducive to higher HR, even though no El Niño event was recorded.

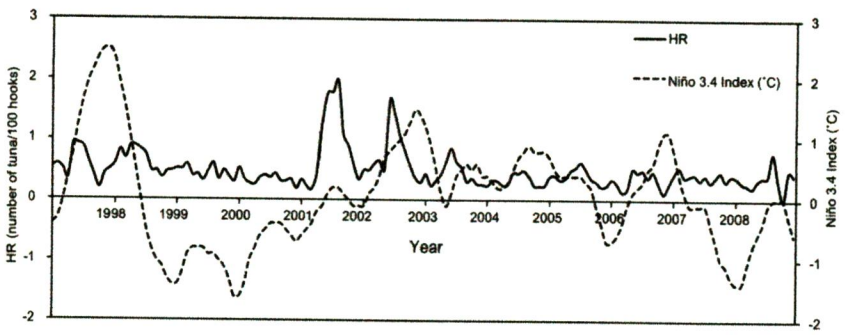

Figure 2. Variability in bigeye tuna catch rates (solid line) and SST anomalies from Niño 3.4 index (dashed line) during the period 1997–2008.

Bigeye tuna catches seem to have declined during the negative Niño 3.4 index (La Niña event) in June 1999 (HR:0.33) and during a normal year in June 2005 (HR: 0.4). The average HR was 0.71 during El Niño, compared to 0.43 during La Niña.

3.2 *Spatial and temporal oceanographic variability*

EOF analysis was applied in the dominant mode forcing and its timescale variability on SSHA, SST, and chl-*a* in order to confirm the HR of bigeye tuna variability due to favourable oceanographic and climatic conditions in the study area. The maps of spatial patterns of the first and second EOF modes of SSHA showed cold water to be located along the southern coast of the Indonesian archipelago, and warm water in the offshore region to create frontal areas along the latitudinal line 10–12° S (Figure 3(*a*) and (*b*)). These EOF modes contributed to 36.5% and 23.5% of total variance and corresponded to interannual and seasonal signals as indicated by the first and second temporal modes, respectively (Figure 4(*a*) and (*b*)).

The maps of spatial patterns of the first and second EOF modes of SST confirmed that the cold water found on the SSHA along the southern coast of the Indonesian archipelago extended further to the offshore areas at 7–13° S, to widen the confluence region southward, meeting warm waters at 7–16° S and 117–125° E (Figure 3(*c*) and (*d*)). These EOF modes contributed to 27.4% and 8.2% of total variance and corresponded to the interannual signal for the first mode and seasonal signal for the second temporal mode (Figure 4(*c*) and (*d*)).

The maps of spatial patterns of the first and second EOF modes of chl-*a* clearly revealed a conduit high chl-*a* concentration along the southern coast of Java and only distributed in the eastern tip of east Java waters, respectively (Figure 3(*e*) and (*f*)). These EOF modes contributed 42.8% and 12.5% of the total variance and

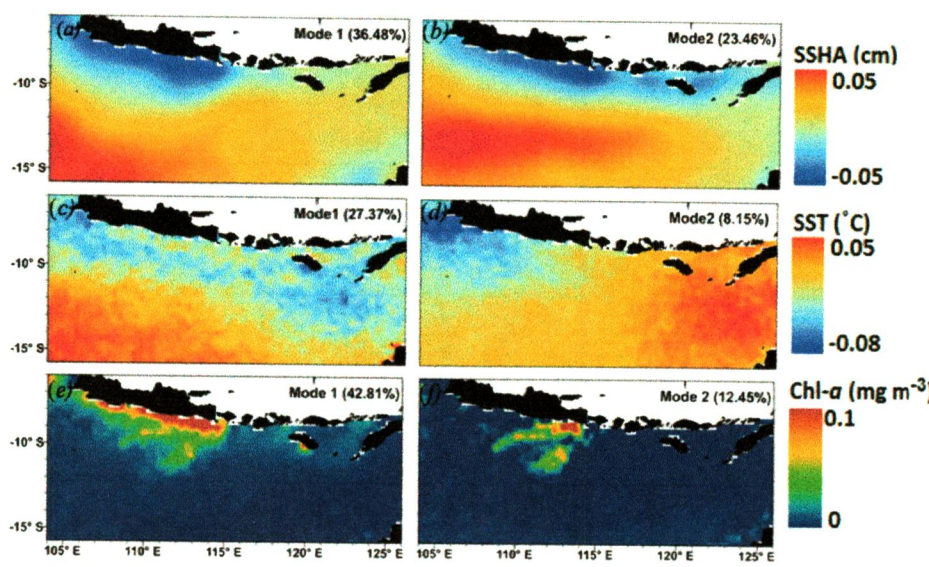

Figure 3. Spatial patterns of EOF modes in the EIO off Java during the period 1997–2008: (*a*) first mode of SSHA, (*b*) second mode of SSHA, (*c*) first mode of SST, (*d*) second mode of SST, (*e*) first mode of chl-*a*, (*f*) second mode of chl-*a*. Scale units are in cm, °C, and mg m^{-3} for SSHA, SST, and chl-*a* data, respectively.

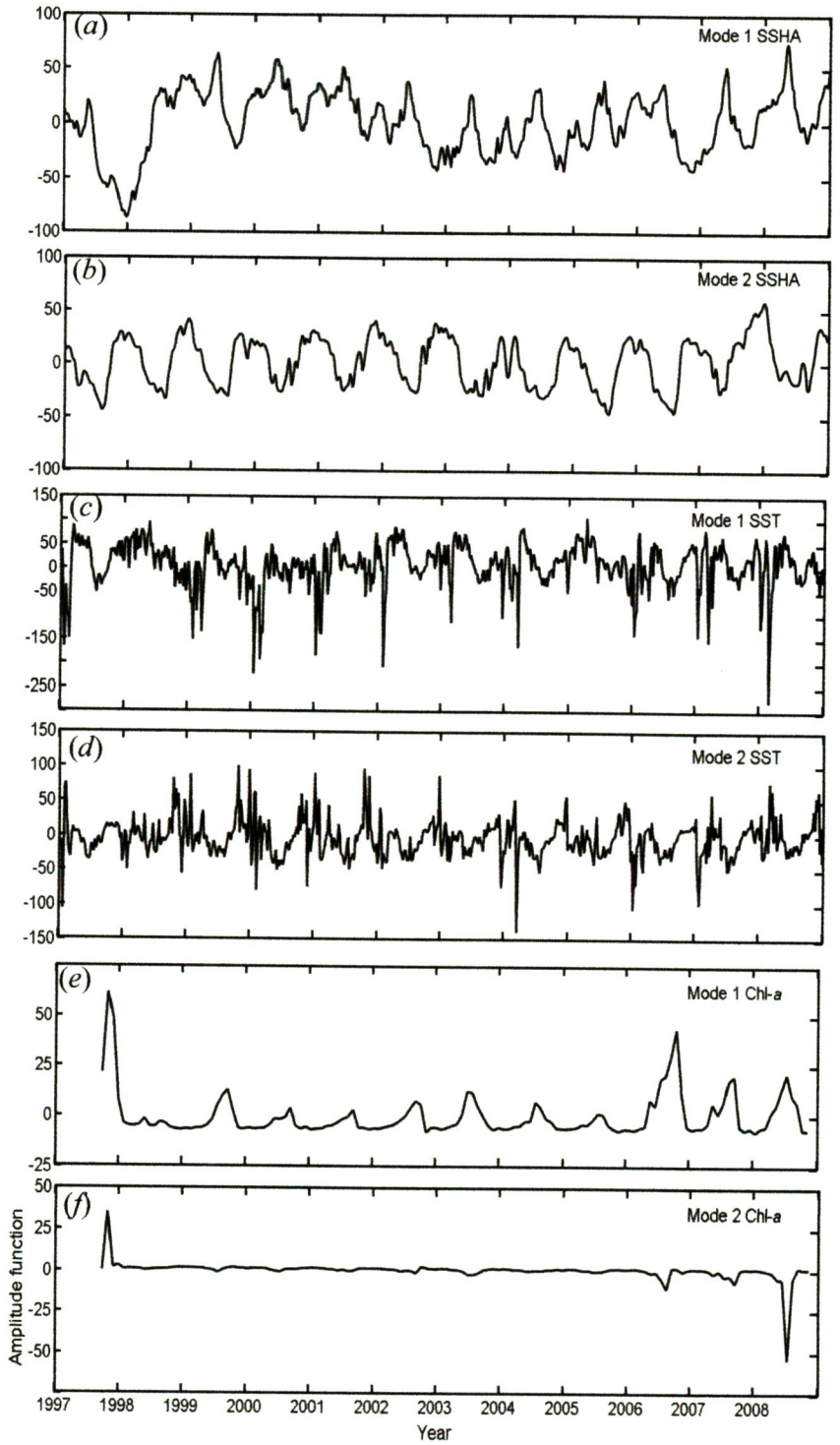

Figure 4. Amplitude function from the temporal mode of EOF analysis in the EIO off Java during the period 1997–2008: (*a*) first mode of SSHA, (*b*) second mode of SSHA, (*c*) first mode of SST, (*d*) second mode of SST, (*e*) first mode of chl-*a*, (*f*) second mode of chl-*a*. The *x*-axis represents year and the *y*-axis amplitude function.

corresponded to the interannual signal for the first mode (Figure 4(*e*)) and decadal signal for the second temporal mode (Figure 4(*f*)), respectively. Total variance of the two major EOF modes of SSHA, SST, and chl-*a* accounted for 59.94%, 35.52%, and 55.26%, respectively.

According to the *in situ* CTD transects and MLD data, the upper thermocline depths during La Niña (February 2000) fluctuated in the range 100–150 m (Figure 5(*a*));

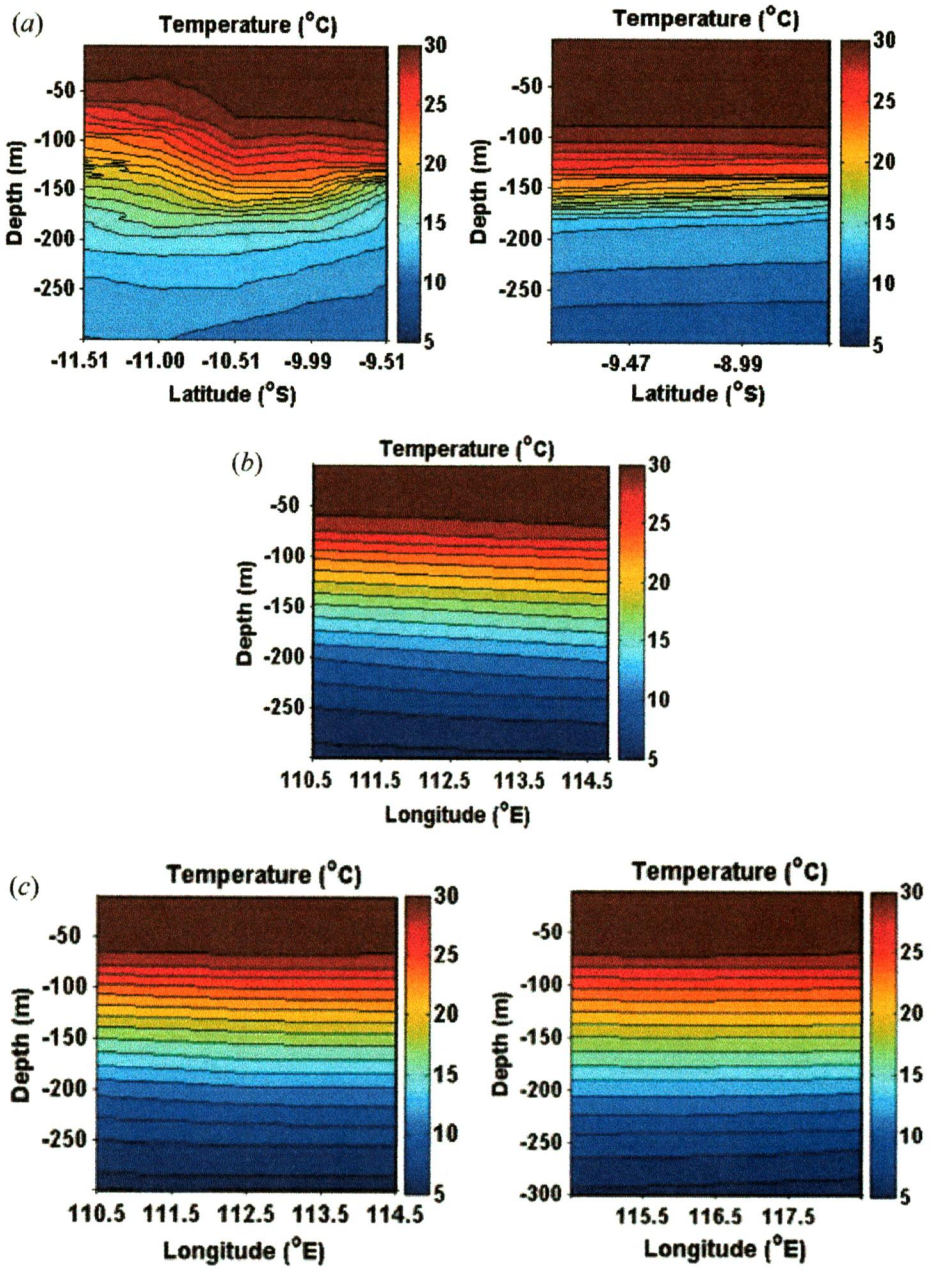

Figure 5. CTD and MLD vertical profile: (*a*) February 2000, (*b*) June 2002, and (*c*) June 2006. The *x*-axis represents the position, and the *y*-axis the depth. Colour bars show the level temperature values (in °C).

conversely during El Niño, the thermocline depth fluctuated between depths of 60 and 90 m (June 2002) (Figure 5(*b*)) and 70 and 90 m (June 2006) (Figure 5(*c*)), respectively.

3.3 *ENSO impact on bigeye tuna hotspots*

In order to understand the HR variations and their association with oceanographic parameters and climate variability, the monthly mean of SSHA, SST, chl-*a*, and EKE were overlaid with the fishing locations and the pixel values sampled (extracted) corresponding to the latitude and longitude. The monthly peak HR in June was overlaid on SSHA, SST, chl-*a*, and EKE maps for the representative years of strong (1997), moderate (2002), and weak (2006) El Niño, strong (1999) La Niña, and normal year (2005), with corresponding HR values of 0.92, 1.66, 0.46, 0.33, and 0.4, respectively (Figure 6). We use only the monthly peak HR value in June for every designated year related to ENSO events, because June represents the most frequent peak of HR during the period 1997–2008.

The results below show the latitude and longitude of fishing locations corresponding to SSHA, SST, chl-*a*, and EKE values. It was confirmed from the four oceanographic variables derived from the satellite images that typically favourable oceanographic conditions related to high potential bigeye tuna catch during El Niño were observed for SSHA ranging from –20 to 20 cm, for SST from 24–27° C, for chl-*a* from 0.1–0.3 mg m^{-3}, and lower EKE of 0–500 cm^2 s^{-2}. Most hotspots of bigeye tuna catch was captured offshore around the confluence region between 11–16° S and 110–118° E. The

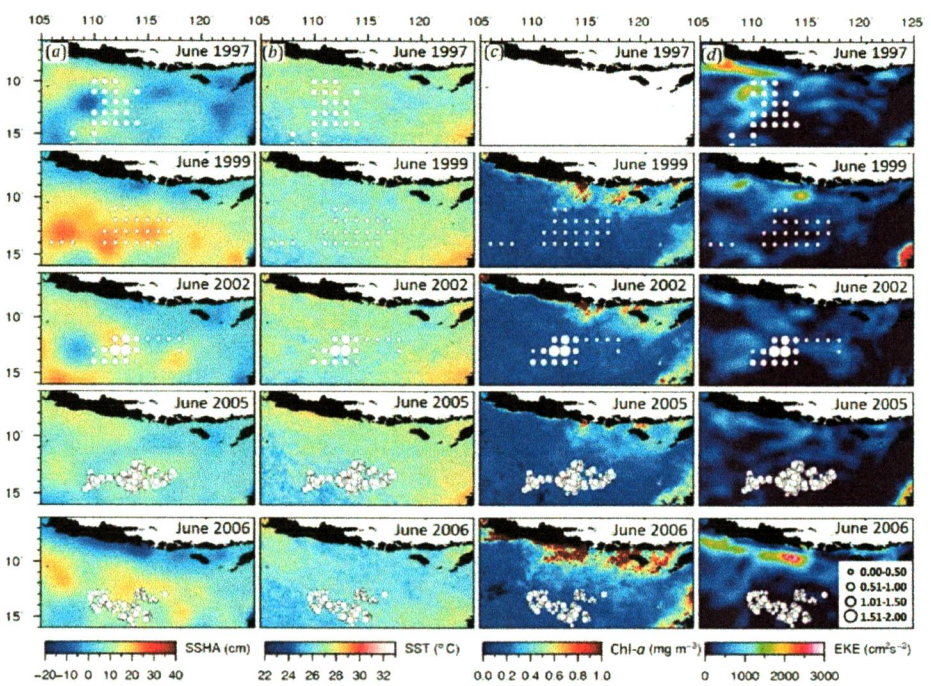

Figure 6. Spatial distribution of bigeye tuna fishing grounds overlaid on monthly mean images for each of the four environmental variables in June 1997 (strong El Niño), 1999 (strong La Niña), 2002 (moderate El Niño), normal condition (2005), and 2006 (weak El Niño) for: (*a*) SSHA, (*b*) SST, (*c*) chl-*a*, (*d*) EKE. Fishing locations with HR values are shown as white dots.

bigeye tuna hotspots in June 1997 (strong El Niño event) were observed between 10–16° S and 108–114° E and showed northward displacement. During a strong La Niña in June 1999, the bigeye tuna fishing locations spread to the western EIO off Java between 11–14° S and 106–117° E. In general, all oceanographic parameters (SSHA, SST, chl-*a*, and EKE) showed the greatest anomalies during the 1997 El Niño. This finding is in agreement with McPhaden (1999), who found that the 1997–1998 El Niño was the strongest on record.

The spatial distribution of bigeye tuna hotspots (HR > 0.5) during 1997–2008 is presented in Figure 1(*b*). HRs changed spatially around 10–16°S and 105–120°E, but they were mostly located in the confluence regions where ITF outflow from Lombok and Ombai Straits and Timor passage, westward Rossby wave propagation, and SEC meet, denoting the most frequent bigeye tuna catch as indicated by blue bars in the offshore region around 12–16° S and 110–118° E.

4. Discussion

The spatial and temporal changes in bigeye tuna catches have shown hotspot locations along the southern coast of the Indonesian archipelago and in the confluence region, and confirmed the similar results as well by EOF analysis. The results confirmed the dependence of bigeye tuna hotspots to oceanographic conditions and increase its magnitude to regional climate condition during El Niño.

Hotspots and catch rates of bigeye tuna varied over a range of time scales and apparently in relation to environmental changes and climatic variability. Changes in oceanographic conditions during ENSO events resulted in perceivable variations in bigeye tuna catches, with increasing HR during El Niño events. HR showed significant increase during El Niño (1997–1998, 2002, and 2006) compared with a La Niña (1999) event and a normal year (2005).

The results indicate that even following single El Niño events such as occurred in June of 2002 and 2006, HR had values of 1.66 and 0.46, respectively, indicative of the fact that favourable oceanographic conditions during the moderate El Niño event in 2002 were more conducive to bigeye tuna catch than during the weak El Niño of 2006. It is noted here that HR values during moderate El Niño in 2002 were much higher than during the strong El Niño in 1997. This could be due to more favourable oceanographic conditions in 2002, where typical cold water – as indicated by negative SSHA (−1 to −20 cm) – and cold SST (24–27°C), followed by a high concentration of chl-*a* (0.1–0.3 mg m^{-3}) and lower EKE values (0–500 cm^2 s^{-2}), were observed along the southern coast of the Indonesian archipelago, with the bigeye tuna hotspots in the confluence region close to high chl-*a* concentration at the eastern tip of east Java waters and frontal warm and cold water areas at 10–12° S and 110° E.

It was also interesting to note that higher HR occurred in the absence of El Niño in 2001 and 2003 due to positive DMI values. IOD analysis is beyond the scope of this study, but it may be important in regard to further studies conducted on Indian Ocean climatic events.

Negative SSHA will push the thermocline upward, nearer the surface, and thus allow bigeye tuna from deeper waters to become more accessible to longline gear. This preferred condition may enhance the potential bigeye tuna habitat, as it apparently did during the 1997–98 and 2002 El Niño events, when increased bigeye tuna catches occurred. These research findings seem to agree with the results of Holland et al. (1992) and Brill (1994), who reported that bigeye tuna move towards cooler habitats to prevent overheating, with

negative values of SSHA indicating that they are attracted only to shallow water when the thermocline is closer to the surface (Arrizabalaga et al. 2008). Howell and Kobayashi (2006) also found the presence of a strong SSHA gradient in the Palmyra region during the 1997/1998 El Niño, coinciding with an increase in the geostrophic (subsurface) flow that may have increased shoaling of longline sets.

ITF is influential in regulating regional SST (Gordon 2005). SST variability is a consequence of the unique position of the Indonesian seas at the confluence of the Pacific and Indian equatorial, and thus the depth of the thermocline and SST in the region can be influenced by remote equatorial winds in both Pacific and Indian Oceans. This mechanism allows the ENSO to influence regional SST (Potemra and Schneider 2007). The shallower thermocline depth during El Niño events is another important factor among oceanographic conditions favourable to identifying bigeye tuna hotspots in the study area. The lower (higher) temperate thermocline relates to the shallower (deeper) one, so that it will reduce (increase) fishing depth in the region. The shallower fishing depth during the strong El Niño event in 2002 could explain the increasing catch rates of bigeye tuna. Conversely, the deeper fishing depth during the La Niña event in1999/2000 could have reduced the impact of SST in regulating the potential fishing catch.

Bigeye tuna fishing locations in June 1999 (during the La Niña event) were observed in the areas of positive SSHA (22–28 cm). The warmer SSHAs were not favourable to bigeye tuna catches in the region, as inferred from the much lower HR of 0.33 during this period. This condition influenced the spatial distribution of bigeye tuna that spread to the western part of the EIO off Java, being less favourable to fishing. This infers that different regional climate events resulted in different oceanographic conditions favourable to bigeye fishing in the study area.

Favourable oceanographic conditions obtained from the satellite images during El Niño are consistent with the EOF results. The spatial patterns of the first and second EOF modes of SSHA, SST, and chl-*a* gave a very typical cold water for SSHA, low SST, and high chl-*a* concentrations along the southern coast of the Indonesian archipelago; and warm water of SSHA, high SST, and much lower chl-*a* concentrations offshore region to create frontal areas along the latitudinal line around 10–12°S (Figure 3). The frontal areas seemed to reveal the confluence region of IOKW and SJC that meet with the outflow of ITF and SEC. The cold water, low SST, and high chl-*a* concentrations along the southern coast of the Indonesian archipelago were likely a manifestation of El Niño events, as shown by the first EOF mode. These typical spatial patterns are consistent with oceanographic conditions during the 1997, 2002, and 2006 El Niño events (Figure 6). These results are consistent with previous findings in the study area using short-term data sets during strong ENSO (1997–2000), where EOF analysis also provides evidence for the effects of the 1997/1998 El Niño event in the EIO off Java with the dominant features being negative SSHA, cold SST, and high chl-*a* concentrations (Syamsuddin et al. 2013). This implies a strong relationship for the El Niño event inducing favourable oceanographic conditions in the EIO off Java. The confluence region where ITF, SEC, SJC, and RW meet in the area 11–16° S and 110–118° E is very important, as the most favourable oceanographic conditions (hotspots) of bigeye tuna catch in the EIO off Java occurred here.

The EOF results further highlight that chl-*a* contributed the highest energy variance, indicating that this parameter is the dominant indicator of the forcing mechanisms responsible for the El Niño event. Our results are consistent with those of Murtugudde et al. (1999), whose study in the Indian Ocean showed that the 1997/1998 El Niño had a direct impact on primary production of the anomalous high values observed in the EIO.

5. Conclusion

The interannual spatial variation of bigeye tuna indicates hotspot locations along the southern coast of the Indonesian archipelago and in the confluence region, and is confirmed by EOF analysis. Therefore, there seem to be strong relationships among ocean climate variability, oceanographic conditions, and bigeye tuna hotspots in the EIO off Java. Major hotspots located off the confluence region and frontal areas around 11–16° S and 110–118° E were found to have the most favourable oceanographic conditions for bigeye tuna fishing in the EIO off Java. These hotspots are markedly dependent on climate, which is more favourable during El Niño events compared with La Niña events and normal years.

EOF analysis further revealed a strong relationship between El Niño events and favourable oceanographic conditions, resulting in significant increases in bigeye tuna catches.

Further research is needed in order to develop a more accurate prediction system to improve and assimilate SINTEX-F (A JAMSTEC running model with the capability of enhanced 3–6-month prediction of ENSO). This will improve our knowledge of fishing ground or hotspot prediction 3–6 months in advance, thus benefitting tuna fishery management in regard to reducing risks and increasing profitability, as well as envisage better social decisions.

Acknowledgements

The authors thank GSFC/DAAC for Chl-*a* and SST data, AVISO for SSHA data, the NOAA Climate Prediction Center for the use of its Niño 3.4 index, and JAMSTEC for the use of Argo float data. The Agency for the Assessment and Application of Technology (BPPT), Indonesia provided the CTD data while the Incorporated Company of Perikanan Nusantara, Indonesia provided the fishery data. This study was supported by the Directorate General of Higher Education of the Republic of Indonesia and the Japan Science Society (JSS) under the Sasagawa Scientific Research Grant [23-744].

Disclosure statement

No potential conflict of interest was reported by the authors.

References

Arrizabalaga, H., J. G. Pereira, F. Royer, B. Galuardi, N. Goñi, I. Artetxe, I. Arregi, and M. Lutcavage. 2008. "Bigeye Tuna (*Thunnus Obesus*) Vertical Movements in the Azores Islands Determined with Pop-Up Satellite Archival Tags." *Fisheries Oceanography* 17: 74–83. doi:10.1111/j.1365-2419.2008.00464.x.

Bigelow, K. A., J. Hampton, and N. Miyabe. 2002. "Application of a Habitat-Based Model to Estimate Effective Longline Fishing Effort and Relative Abundance of Pacific Bigeye Tuna (*Thunnus Obesus*)." *Fisheries Oceanography* 11: 143–155. doi:10.1046/j.1365-2419.2002.00196.x.

Bjornsson, H., and S. A. Venegas. 1997. "A Manual for EOF and SVD Analyses of Climatic Data." *CCGCR Report* 97-1: 52.

Briand, K., M. Brett, and L. Patrick. 2011. "A Study on the Variability of Albacore (*Thunnus Alalunga*) Longline Catch Rates in the Southwest Pacific Ocean." *Fisheries Oceanography* 20: 517–529. doi:10.1111/j.1365-2419.2011.00599.x.

Brill, R. W. 1994. "A Review of Temperature and Oxygen Tolerance Studies of Tunas Pertinent to Fisheries Oceanography, Movement Models and Stock Assessments." *Fisheries Oceanography* 3: 204–216. doi:10.1111/fog.1994.3.issue-3.

Ffield, A., K. Vranes, A. L. Gordon, R. D. Susanto, and S. L. Garzoli. 2000. "Temperature Variability within Makassar Strait." *Geophysical Research Letter* 27: 237–240. doi:10.1029/1999GL002377.

Gordon, A. L. 2005. "Oceanography of the Indonesian Seas and Their Throughflow." *Oceanography* 18: 13–13. doi:10.5670/oceanog.

Holland, K. N., R. W. Brill, R. K. C. Chang, and J. R. Sibert. 1992. "Physiological and Behavioral Thermoregulation in Bigeye Tuna (*Thunnus Obesus*)." *Nature* 358: 410–412. doi:10.1038/358410a0.

Howell, E. A., D. R. Hawn, and J. J. Polovina. 2010. "Spatiotemporal Variability in Bigeye Tuna (*Thunnus Obesus*) Dive Behavior in the Central North Pacific Ocean." *Progress in Oceanography* 86: 81–93. doi:10.1016/j.pocean.2010.04.013.

Howell, E. A., and D. R. Kobayashi. 2006. "El Niño Effects in the Palmyra Atoll Region: Oceanographic Changes and Bigeye Tuna (*Thunnus Obesus*) Catch Rate Variability." *Fisheries Oceanography* 15: 477–489. doi:10.1111/j.1365-2419.2005.00397.x.

Iida, T., and S. Saitoh. 2007. "Temporal and Spatial Variability of Chlorophyll Concentrations in the Bering Sea Using Empirical Orthogonal Function (EOF) Analysis of Remote Sensing Data." *Deep Sea Research Part II: Topical Studies in Oceanography* 54: 2657–2671. doi:10.1016/j.dsr2.2007.07.031.

Iskandar, I., A. Rao, and T. Tozuka. 2008. "Chlorophyll-a Bloom along the Southern Coasts of Java and Sumatra during 2006." *International Journal of Remote Sensing* 30: 663–671. doi:10.1080/01431160802372309.

ISSF. 2012. *ISSF Stock Status Ratings-2012, Status of the World Fisheries for Tuna*. International Seafood Sustainability Foundation (ISSF) Technical Report. 1–88. Washington, DC: International Seafood Sustainability Foundation.

Kelly, K. A. 1988. "Comment on "Empirical Orthogonal Function Analysis of Advanced Very High Resolution Radiometer Surface Temperature Patterns in Santa Barbara Channel" by G.S.E. Lagerloef and R.L." *Bernstein. Journal of Geophysical Research* 93: 15753–15754. doi:10.1029/JC093iC12p15753.

Lehodey, P. 2001. "The Pelagic Ecosystem of the Tropical Pacific Ocean: Dynamic Spatial Modelling and Biological Consequences of ENSO." *Progress in Oceanography* 49: 439–468. doi:10.1016/S0079-6611(01)00035-0.

Lehodey, P., M. Bertignac, J. Hampton, A. Lewis, and J. Picaut. 1997. "El Niño Southern Oscillation and Tuna in the Western Pacific." *Nature* 389: 715–718. doi:10.1038/39575.

McPhaden, M. J. 1999. "Genesis and Evolution of the 1997–98 El Niño." *Science* 283: 950–954. doi:10.1126/science.283.5404.950.

Miyake, M., P. Guillotreau, C.-H. Sun, and G. Ishimura. 2010. "Recent Developments in the Tuna Industry: Stocks, Fisheries, Management, Processing, Trade and Markets." *FAO Fisheries and Aquaculture Technical Paper* 543: 1–25.

Mohri, M., and T. Nishida. 1999. "Distribution of Bigeye Tuna and Its Relationship to the Environmental Conditions in the Indian Ocean Based on the Japanese Longline Fisheries Information." *IOTC Proceedings* 2: 221–230.

Murtugudde, R. G., S. R. Signorini, J. R. Christian, A. J. Busalacchi, C. R. Mcclain, and J. Picaut. 1999. "Ocean Color Variability of the Tropical Indo-Pacific Basin Observed by Seawifs during 1997–1998." *Journal of Geophysical Research* 104: 18351–18366. doi:10.1029/1999JC900135.

Pepperell, J. 2010. *Fishes of the Open Ocean*, 75–80. Chicago: The University of Chicago Press.

Polovina, J. J., and E. A. Howell. 2005. "Ecosystem Indicators Derived from Satellite Remotely Sensed Oceanographic Data for the North Pacific." *ICES Journal of Marine Science* 62: 319–327. doi:10.1016/j.icesjms.2004.07.031.

Potemra, J. T., and N. Schneider. 2007. "Interannual Variations of the Indonesian Throughflow." *Journal of Geophysical Research* 112: 1–13. doi:10.1029/2006JC003808.

Rao, S. A., J. J. Luo, K. B. Swadhin, and T. Yamagata. 2009. "Generation and Termination of Indian Ocean Dipole Events in 2003, 2006 and 2007." *Climate Dynamics* 33: 751–767. doi:10.1007/s00382-008-0498-z.

Robinson, I. S. 2004. *Measuring Oceans from Space: The Principles and Methods of Satellite Oceanography*, 669 p. Chichester: Praxis Publishing, UK.

Saji, N. H., B. N. Goswami, P. N. Vinayachandran, and T. Yamagata. 1999. "A Dipole Mode in the Tropical Indian Ocean." *Nature* 401: 360–363. doi:10.1038/43854.

Sprintall, J., J. C. Chong, F. Syamsudin, W. Morawit, S. Hautala, N. Bray, and S. E. Wijffels. 1999. "Dynamics of the South Java Current in the Indo-Australian Basin." *Geophysical Research Letter* 26: 2493–2496. doi:10.1029/1999GL002320.

Sprintall, J., S. E. Wijffels, R. Molcard, and I. Jaya. 2009. "Direct Estimates of the Indonesian Throughflow Entering the Indian Ocean: 2004–2006." *Journal of Geophysical Research* 114: 1–19. doi:10.1029/2008JC005257.

Sprintall, J., S. E. Wijffels, R. Molcard, and I. Jaya. 2010. "Direct Evidence of the South Java Current System in Ombai Strait." *Dynamics of Atmospheres and Oceans* 50: 140–156. doi:10.1016/j.dynatmoce.2010.02.006.

Susanto, R. D., T. S. Moore, and J. Marra. 2006. "Ocean Color Variability in the Indonesian Seas during the Seawifs Era." *Geochemistry Geophysics Geosystems* 7: 1599–1602. doi:10.1029/2005GC001009.

Syamsuddin, M. L., S. Saitoh, T. Hirawake, S. Bachri, and A. B. Harto. 2013. "Effects of El Niño-Southern Oscillation Events on Catches of Bigeye Tuna (*Thunnus Obesus*) in the Eastern Indian Ocean off Java." *Fishery Bulletin* 111: 175–188. doi:10.7755/FB.

Syamsudin, F., A. Kaneko, and D. B. Haidgovel. 2004. "Numerical and Observational Estimates of Indian Ocean Kelvin Wave Intrusion into Lombok Strait." *Geophysical Research Letter* 31: 1–4. doi:10.1029/2004GL021227.

Torres-Orozco, E., A. Muhlia-Melo, A. Trasvina, and S. Ortega-Garcia. 2006. "Variation in Yellowfin Tuna (*Thunnus Albacares*) Catches Related to El Niño-Southern Oscillation Events at the Entrance to the Gulf of California." *Fishery Bulletin* 104: 197–203.

Yoder, J. A., and M. A. Kennely. 2003. "Seasonal and ENSO Variability in Global Ocean Phytoplankton Chlorophyll Derived from 4 Years of Seawifs Measurements." *Global Biogeochemical Cycles* 17: 1112p. doi:10.1029/2002GB001942.

Zhou, L., R. Murtugudde, and M. Jochum. 2008. "Dynamics of the Intraseasonal Oscillations in the Indian Ocean South Equatorial Current." *Journal of Physical Oceanography* 38: 121–132. doi:10.1175/2007JPO3730.1.